Nuclear Physics A203 (1974) 105—120;

PROPERTIES OF SINGLE-PARTICLE STATES IN THE ^{208}Pb REGION

S. REICH, H. M. SOFÍA and D. R. BÈS †

Comisión Nacional de Energía Atómica, Departamento de Física Nuclear, Buenos Aires, Argentina

Received 11 February 1974
(Revised 10 June 1974)

Abstract: The properties of single-particle states in the ^{208}Pb region are obtained by subtracting from the empirical values the dressing effects of the multipole particle-hole and pairing phonons. Use is made of the particle-vibration formalism. Single-particle energies, one-body transfer spectroscopic factors and effective quadrupole charges are examined within this framework.

1. Introduction

It has become apparent [1]) that the best region for the application of the shell model lies in the neighbourhood of ^{208}Pb. In addition, this region represents one of the last known points for the extrapolation of single-particle properties in the search for new islands of stability. Therefore, it is important to determine the properties of the single-particle states in this region as accurately as possible. This has been done, for instance, by optimizing the choice of the parameters in a Saxon-Woods potential [2]). The single-particle wave functions thus determined have been used, for instance, to obtain the renormalized value of the electric charge and g-factors corresponding to different multipole transitions [3]).

However, it has also been recognized that in this region there are states with conspicuous collective properties, such as the lowest $j^\pi = 3^-$ and 0^+ excited states in ^{208}Pb. It is clear that the presence of these collective states may induce admixtures in the single-particle states through the particle-vibration interaction. A well known case [4]) is the $j^\pi = \frac{1}{2}^-$ state in ^{209}Bi. In this paper we attempt to extract the "bare" single-particle properties of the states in ^{207,209}Pb, ^{207}Tl and ^{209}Bi. The difference between the present calculation and some of the results reported in ref. [4]) lies in the fact that we consider the effects associated with the pairing forces, but we do not explicitly include effects associated with the continuum, since we use harmonic oscillator wave functions. Within this limitation, we focus our attention on the properties of the "bare" single-particle states. Therefore, from the point of view of the energies, this paper follows a line similar to refs. [5]) for spherical nuclei or to refs. [6]) for deformed nuclei. With respect to the transition rates, we examine to which extent the conclusions of ref. [3]) are modified by the presence of admixtures in the predominant

† Fellow of the Consejo Nacional de Investigaciones Científicas y Técnicas.

single-particle states, and we analyze experimental evidence for transfer processes between these states [7]).

2. Review of the formalism

We shall use a similar formalism as in ref. [8]). Therefore, we have an unperturbed Hamiltonian consisting of independent particles and independent phonons. Both particle-hole ($\alpha = 0$) and pairing ($\alpha = \pm 2$) bosons are included:

$$H = \sum_j \varepsilon_j c_j^+ c_j + \sum_{\alpha\lambda} W(\alpha, \lambda) \Gamma^+(\alpha, \lambda) \Gamma(\alpha, \lambda). \tag{1}$$

Here j and λ denote not only the angular momentum but also the remaining variables that are necessary in order to specify the state. For single-particle states above (below) the Fermi level, j will be replaced by $k(i)$. The operators c_j^+ and $\Gamma^+(\alpha, \lambda)$ create a particle and a boson, respectively, while the ε_j and $W(\alpha, \lambda)$ denote the single-particle energies and boson frequencies, respectively.

The interaction depends linearly either on the particle-hole or on the pairing collective variables. All possible time-ordering of the vertices that appear diagrammatically in perturbation theory are to be included [9]). This interaction takes care of violations of the Pauli principle and in general of spurious effects associated with the over-completeness of the basis [8-10]):

$$H_{\text{int}} = -\sum_{\alpha\lambda} \Lambda(\alpha, \lambda) \{\Gamma^+(\alpha, \lambda) + (-)^\lambda \Gamma(-\alpha, \lambda)\} Q^+(\alpha, \lambda), \tag{2}$$

where the 2λ pole operators are defined as

$$Q(0, \lambda) = \frac{-1}{\sqrt{2\lambda+1}} \sum_{k,i} M(ki, \lambda) \{\beta^+(ki; 0\lambda) + (-)^\lambda \beta(ki; 0\lambda)\},$$

$$Q(2, \lambda) = \frac{-2}{\sqrt{2\lambda+1}} \left\{ \sum_{k_1 \geqq k_2} \frac{M(k_1 k_2, \lambda)}{(1+\delta_{12})^{\frac{1}{2}}} \beta^+(k_1 k_2; 2\lambda) + \sum_{i_1 \geqq i_2} \frac{M(i_1 i_2, \lambda)}{(1+\delta_{12})^{\frac{1}{2}}} \beta(i_1 i_2; -2\lambda) \right\},$$

$$Q(-2, \lambda) = \frac{-2}{\sqrt{2\lambda+1}} \left\{ \sum_{i_1 \geqq i_2} \frac{M(i_1 i_1, \lambda)}{(1+\delta_{12})^{\frac{1}{2}}} \beta^+(i_1 i_2; -2\lambda) + \sum_{k_1 \geqq k_2} \frac{M(k_1 k_2, \lambda)}{(1+\delta_{12})^{\frac{1}{2}}} \beta(k_1 k_2; 2\lambda) \right\}, \tag{3}$$

where

$$\begin{aligned} M(j_1 j_2; \lambda) &= \langle j_1 || f_\lambda(r) Y_\lambda || j_2 \rangle i^{l_{j_2} - l_{j_1} + \lambda}, \\ \beta^+(ki, 0\lambda) &= \{c_k^+ c_i\}^\lambda, \\ \beta^+(k_1 k_2, 2\lambda) &= (1+\delta_{12})^{-\frac{1}{2}} \{c_{k_2}^+ c_{k_2}\}^\lambda, \\ \beta^+(i_1 i_2, -2\lambda) &= (1+\delta_{12})^{-\frac{1}{2}} \{c_{i_1} c_{i_2}\}^\lambda. \end{aligned} \tag{4}$$

The coupling strengths $\Lambda(\alpha, \lambda)$ are determined by the boson frequencies and single-particle energies through the RPA relations

$$\Lambda(0,\lambda) = \left\{\sum_{k,i} |M(ki,\lambda)|^2 \left(\frac{1}{\{\varepsilon_k - \varepsilon_i - W(0,\lambda)\}^2} - \frac{1}{\{\varepsilon_k - \varepsilon_i + W(0,\lambda)\}^2}\right)\right\}^{-\frac{1}{2}},$$

$$\Lambda(\pm 2,\lambda) = \sqrt{2}\left(\pm \sum_{k_1,k_2} \frac{|M(k_1 k_2,\lambda)|^2}{\{\varepsilon_{k_1} + \varepsilon_{k_2} \mp W(\pm 2,\lambda)\}^2} \mp \sum_{i_1,i_2} \frac{|M(i_1 i_2,\lambda)|^2}{\{-\varepsilon_{i_1} - \varepsilon_{i_2} \pm W(\pm 2,\lambda)\}^2}\right)^{-\frac{1}{2}}. \tag{5}$$

In lowest order, the corrections to the single-particle energies are given by graphs of fig. 1:

$$E_{k_1} - \varepsilon_{k_1} = \sum_{\lambda} \frac{2\lambda+1}{2k_1+1} \{\Lambda(0,\lambda)\}^2 \left(\sum_i \frac{|M(k_1 i,\lambda)|^2}{W(0,\lambda) - \varepsilon_i + \varepsilon_{k_1}} - \sum_{k_2} \frac{|M(k_1 k_2,\lambda)|^2}{W(0,\lambda) + \varepsilon_{k_2} - \varepsilon_{k_1}}\right)$$
$$+ \sum_{\lambda} \frac{2\lambda+1}{2k_1+1} \left(\sum_{k_2} \frac{|\Lambda(-2\lambda) M(k_1 k_2,\lambda)|^2}{W(-2,\lambda) + \varepsilon_{k_1} + \varepsilon_{k_2}} - \sum_i \frac{|\Lambda(2\lambda) M(k_1 i,\lambda)|^2}{W(2,\lambda) - \varepsilon_i - \varepsilon_{k_1}}\right). \tag{6}$$

There are two kinds of processes involved in (6): (i) Those represented by graphs which have a 2p-1h state as intermediate state. They tend to repel the single-particle states from the intermediate states and, consequently, their contributions have a

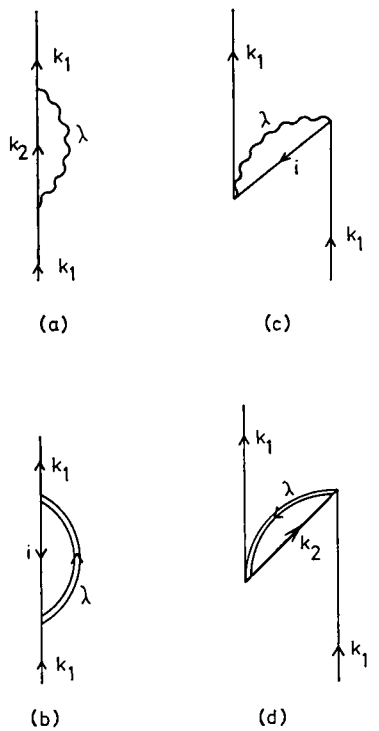

Fig. 1. The graphs representing the four processes giving rise to eq. (6).

negative sign. (ii) Those graphs which arise because of ground state correlations. The presence of the odd-particle tends to destroy these correlations and, therefore, they yield a positive contribution to the single-particle energy. Corresponding processes exist for the single-hole states. Similarly the particle-hole excitation energies are decreased by processes of type (i) and are increased by processes of type (ii).

Our aim is to determine the bare single-particle energies which appear in the right hand side of eq. (6). We assume that the experimental excitation energies are to be substituted in the left hand side. The frequency $W(0, \lambda)$ of the particle-hole boson may be taken directly from experiment, since these energies are affected only in fourth order in Λ and thus they are correct to the order of perturbation theory which has been taken into account in (6). The usual procedure for the determination of $W(2, 0)$ is based on appropriate differences between the binding energies of $^{206-210}$Pb (neutron case) and of ^{206}Hg, ^{208}Pb and ^{210}Po (proton case). However, this procedure offers some uncertainty since these differences only eliminate the binding energies terms which are linear in the number of particles. Therefore, for instance, residual Coulomb and/or isospin contributions subsist in the resultant pairing energies.

In order to eliminate these effects we should use energy differences between levels belonging to the same nucleus. For instance, we may use the experimental excitation energy $W(2, 0)+W(-2, 0)$ of the two-pairing-phonon state in ^{208}Pb, which is also unaffected in second order of perturbation theory. We could thus determine the strength of the pairing force associated with the $\lambda = 0$ channel through the RPA dispersion relation and, at the same time, calculate the remaining properties of the $\alpha = \pm 2$, $\lambda = 0$ phonons. Subsequently, we calculate $W(2, \lambda)$ from the empirical differences $W(2, \lambda)-W(2, 0)$ and the value of $W(2, 0)$ which has been previously obtained. The inconvenience with this method lies in the fact that the energy difference $\Delta W(\alpha = 2, \lambda = 8) = 2\varepsilon_{g_{\frac{9}{2}}} - W(2, 8)$ is smaller than the uncertainty in the values of the terms which have to be subtracted from each other, and therefore the resulting particle-phonon coupling constants corresponding to the pairing phonons with high λ cannot be trusted.

A third possibility consists of fixing the value of $\Delta W(2, 8)$ from the beginning. We may use, for instance, the result of a theoretical calculation. Subsequently, we determine the difference $\Delta W(2, \lambda)$, $\lambda \neq 8$, from the experimentally known excitation energies $W(2, 8)-W(2, \lambda)$. We have adopted this third method and we have verified that the properties of the more important $\alpha = 2$ phonons (low values of λ) are not significantly different for two different reasonable values of $\Delta W(2, 8)$ (0.10 MeV and 0.05 MeV, respectively).

If a particle state is sufficiently close to a particle-phonon state, perturbation theory may not converge. Therefore, we have made the decision that if the amplitude of one (or several) particle-boson state in an otherwise predominant single-particle state exceeds the value 0.5, we perform a diagonalization in a restricted basis consisting of the particle state and that (those) particle-boson state. The contribution of the

last one in (6) is replaced by the energy difference between the root corresponding to the largest amplitude of the particle state and the unperturbed position of this state.

3. Determination of the bare single-particle energies

The left hand side of eq. (6) (i.e., the experimental energies of the predominantly single-particle or single-hole states) is given in ref. [2]). The collective parameters to be used in the right hand side are discussed in the previous section. In the neutron (proton) case, we use as minimization variables the "bare" energy differences $\varepsilon_k - \varepsilon_{k0}$ between the seven (six) particle states above the Fermi level and the differences $\varepsilon_{i0} - \varepsilon_i$ between the six (five) hole states below the Fermi level, plus the smallest "bare" distance $\varepsilon_{k0} - \varepsilon_{i0}$ between particles and holes. We include in (6) these thirteen single-neutron states (eleven single-proton states) plus the collective phonons that appear in the low energy spectrum of ^{208}Pb (table 1).

TABLE 1

The values of the coupling constant $\Lambda(\alpha, \lambda)$ in units of $(m\omega/\hbar)^{\frac{1}{2}\lambda}$ MeV

α	λ	τ_z	Exp single-particle energies	Bare single-particle energies	
				$r^4 Y_{4,0}$ $\Delta W(2, 8) = 0.05$	$r^2 Y_{4,0}$ $\Delta W(2, 8) = 0.05$
0	3	0	0.041	0.040	0.041
0	5	0	0.0011	0.00043	0.00036
0	2	0	0.154	0.137	0.141
0	4	0	0.011	0.0099	0.115
2	0	1	2.14	2.05	2.05
−2	0	1	1.89	1.69	1.59
2	2	1	0.11	0.10	0.10
−2	2	1	0.10	0.096	0.094
2	4	1	0.0059	0.0050	0.050
−2	4	1	0.0048	0.0039	0.051
2	6	1	0.00038	0.00028	0.00028
−2	6	1	0.00037	0.00024	0.00021
2	8	1	0.00002	0.00001	0.00001
−2	8	1	0.00001	0.00001	0.00001
2	0	−1	2.38	2.40	2.40
−2	0	−1	2.28	2.25	2.14
2	2	−1	0.10	0.092	0.092
−2	2	−1	0.092	0.085	0.081
2	4	−1	0.0068	0.0054	0.041
−2	4	−1	0.0077	0.0075	0.059
2	6	−1	0.00068	0.00051	0.00051
−2	6	−1	0.00044	0.00041	0.00041
2	8	−1	0.0004	0.00002	0.00002
−2	8	−1	0.00002	0.00002	0.00002

The different columns are obtained by replacing in (5) the experimental single-particle energies or the bare single-particle energies corresponding to the hexadecapole field with a r^4 radial dependence ($\Delta W(2, 8) = 0.05$ MeV) and with a r^2 radial dependence ($\Delta W(2, 8) = 0.05$ MeV), respectively.

TABLE 2a

The single-neutron bare and perturbed energy differences $\varepsilon_k - \varepsilon_{\frac{9}{2}}$ ($\varepsilon_k > \varepsilon_F$), $\varepsilon_{\frac{1}{2}} - \varepsilon_l$ ($\varepsilon_l < \varepsilon_F$) and $\varepsilon_{\frac{9}{2}} - \varepsilon_{\frac{1}{2}}$ for the two different radial dependences of the hexadecapole field (in MeV)

Single-neutron states	Exp energies	$r^4 Y_{4,0}$ $\Delta W(2, 8) = 0.05$ MeV		$r^2 Y_{4,0}$ $\Delta W(2, 8) = 0.05$ MeV	
		bare	perturbed	bare	perturbed
$f_{\frac{5}{2}}$	0.57	0.62	0.57	0.74	0.56
$p_{\frac{3}{2}}$	0.90	0.98	0.88	1.06	0.88
$i_{13/2}$	1.63	1.71	1.53	1.77	1.51
$f_{\frac{7}{2}}$	2.34	3.36	2.23	3.61	2.24
$h_{\frac{9}{2}}$	3.43	4.08	3.39	4.25	3.53
$i_{11/2}$	0.78	0.58	0.77	0.59	0.77
$j_{15/2}$	1.43	1.68	1.49	1.67	1.43
$d_{\frac{5}{2}}$	1.57	1.96	1.58	2.09	1.61
$s_{\frac{1}{2}}$	2.04	3.00	2.04	1.93	2.05
$g_{\frac{7}{2}}$	2.50	2.90	2.53	2.91	2.51
$d_{\frac{3}{2}}$	2.54	3.66	2.48	3.11	2.52
$\varepsilon_{\frac{9}{2}} - \varepsilon_{\frac{1}{2}}$		3.21	2.93	3.19	2.92

TABLE 2b

The single-proton bare and perturbed energy differences $\varepsilon_k - \varepsilon_{\frac{9}{2}}$ ($\varepsilon_k > \varepsilon_F$), $\varepsilon_{\frac{1}{2}} - \varepsilon_l$ ($\varepsilon_l < \varepsilon_F$) and $\varepsilon_{\frac{9}{2}} - \varepsilon_{\frac{1}{2}}$ for the two different radial dependences of the hexadecapole field (in MeV)

Single-proton states	Exp energies	$r^4 Y_{4,0}$ $\Delta W(2, 8) = 0.05$ MeV		$r^2 Y_{4,0}$ $\Delta W(2, 8) = 0.05$ MeV	
		bare	perturbed	bare	perturbed
$d_{\frac{5}{2}}$	0.35	0.41	0.35	0.60	0.35
$h_{11/2}$	1.34	1.60	1.36	1.71	1.37
$g_{\frac{7}{2}}$	1.67	2.48	1.65	3.15	1.68
$d_{\frac{3}{2}}$	3.48	4.29	3.40	4.37	3.54
$f_{\frac{5}{2}}$	0.89	1.21	0.90	1.26	0.90
$i_{13/2}$	1.60	1.97	1.60	1.99	1.60
$f_{\frac{7}{2}}$	2.81	4.17	2.95	4.18	2.74
$p_{\frac{3}{2}}$	3.11	4.52	3.04	4.55	3.15
$p_{\frac{1}{2}}$	3.62	4.46	2.84	4.55	3.16
$\varepsilon_{\frac{9}{2}} - \varepsilon_{\frac{1}{2}}$		3.89	3.95	3.76	3.79

Since the phonon energies are taken from experimental results, we use the RPA formalism only to obtain the coupling strengths $\Lambda(\alpha, \lambda)$. In the summation (5) we allow all the single-particle states corresponding to the neutron harmonic oscillator shells with $N \leqq 12$ and proton shells with $N \leqq 10$. However, the results are not sensitive to the highly excited states that we include in (5), since their contribution is inversely proportional to the cube of the excitation energy. We also let vary in (5)

the same single-particle energies that are included in (6), while the remaining single-particle energies are obtained from a Nilsson spherical potential.

The neutron and proton variables are coupled through the expression for the interaction parameters $A(0, \lambda)$ corresponding to the particle-hole phonons. In order to decrease the number of minimization variables, we minimize first only with respect to the neutron single-particle energies. In a second step we vary the proton energies, keeping constant the neutron energies which have been previously determined. Self-consistency is achieved after a few iterations. The resultant values of $A(\alpha, \lambda)$ are listed in table 1.

TABLE 3

The displacement of the energy ΔE for the $g_{\frac{9}{2}}$ single-neutron states in second order of perturbation theory

Graphs	1a			1b			1c			1d		
	l_j	α, λ	ΔE	l_j	α, λ	ΔE	l_j	α, λ	ΔE	l_j	α, λ	ΔE
$p_{\frac{1}{2}}$	$p_{\frac{3}{2}}$	0, 2	−0.16				$d_{\frac{5}{2}}$	0, 3	0.13	$p_{\frac{1}{2}}$	2, 0	0.07
	$f_{\frac{5}{2}}$	0, 2	−0.22				$g_{\frac{7}{2}}$	0, 3	0.16	$p_{\frac{3}{2}}$	2, 2	0.06
	$h_{\frac{9}{2}}$	0, 4	−0.10							$f_{\frac{5}{2}}$	2, 2	0.08
	$f_{\frac{7}{2}}$	0, 4	−0.17							$h_{\frac{9}{2}}$	2, 4	0.02
										$f_{\frac{7}{2}}$	2, 4	0.04
$g_{\frac{9}{2}}$	$f_{\frac{5}{2}}$	0, 3	−0.19	$i_{\frac{13}{2}}$	2, 2	−0.05	$f_{\frac{7}{2}}$	0, 3	0.04	$g_{\frac{9}{2}}$	−2, 0	0.03
	$g_{\frac{9}{2}}$	0, 2	−0.12	$i_{\frac{13}{2}}$	2, 4	−0.02	$p_{\frac{3}{2}}$	0, 3	0.08	$g_{\frac{9}{2}}$	−2, 2	0.04
	$d_{\frac{5}{2}}$	0, 2	−0.07				$i_{\frac{13}{2}}$	0, 2	0.04	$d_{\frac{5}{2}}$	−2, 2	0.02
	$g_{\frac{9}{2}}$	0, 4	−0.10				$i_{\frac{13}{2}}$	0, 4	0.04			
	$d_{\frac{5}{2}}$	0, 4	−0.06									
	$s_{\frac{1}{2}}$	0, 4	−0.05									
	$g_{\frac{7}{2}}$	0, 4	−0.02									
	$d_{\frac{3}{2}}$	0, 4	−0.02									

The graphs are labelled as in fig. 1. The intermediate state is identified in the first and second columns corresponding to each graph. The displacement ΔE is given in MeV. Only $|\Delta E| \geqq 0.02$ MeV have been included.

We use the adjective "bare" to denote the properties of the single-particle states once we remove the effects of the phonons that are listed in table 1. However, it is obvious that the particles are not yet free nucleons, because of the existence of higher energy bosons (giant resonances) and short range repulsive correlations.

The reduced matrix elements $M(j_1 j_2, \lambda)$ are calculated using harmonic oscillator wave functions and the radial dependence r^λ for $f_\lambda(r)$ †. As in ref. [8]) the resultant numbers are multiplied by the factor $13/(N_1+N_2+3)$, in order to decrease the dependence of the harmonic oscillator matrix elements upon the main quantum number N.

† However, we have tried also dependence r^2 for the $\lambda = 4$ phonon. See the discussion in the following.

A least-square fit for the relative excitation energies has been performed with the aid of the routine MINUIT. The resulting bare and dressed energies are given in tables 2a and 2b.

We note that the bare single-particle states are more spread in energy than the dressed ones.

Table 3 illustrates the contributions of the displacements corresponding to the $p_{\frac{1}{2}}$ and $g_{\frac{9}{2}}$ neutron states. We verify that those graphs corresponding to a 2p-1h intermediate state (graphs 1a, 1b) yield a negative contribution to the single-particle energy, while those representing a partial cancellation of the ground state correlations (graphs 1c, 1d) give a positive contribution. For $p_{\frac{1}{2}}$ both effects have the same absolute value, while in the $g_{\frac{9}{2}}$ case the first effect predominates. This is the reason why the displacement of the $g_{\frac{9}{2}}$ is larger than the one corresponding to the $p_{\frac{1}{2}}$ level, although there are twice as many contributions greater than 0.10 MeV for the $p_{\frac{1}{2}}$ than for the $g_{\frac{9}{2}}$ level.

TABLE 4

The optimum depth parameters of the Saxon-Woods potential (eq. (7)) in order to fit the experimental and single-particle energies

	Exp single-particle energies	Bare single-particle energies	
		$r^4Y_{4,0}$ $\Delta W(2, 8) = 0.05$ MeV	$r^2Y_{4,0}$ $\Delta W(2, 8) = 0.05$ MeV
V_0 (n)	44.1	44.6	45.0
$V_{s.o.}$ (n)	32.0	33.7	32.5
V_0 (p)	58.0	58.7	58.9
$V_{s.o}$ (p)	32.0	28.4	28.5

There are several cases such that the contributions from perturbation theory are replaced by those coming from a diagonalization. These cases correspond always to processes of the type graph 1a and involve the $\lambda = 3$, 4 particle-hole phonons.

Since we do not have sufficient experience, for instance, on the radial dependence of the hexadecapole field, we have performed another search for the bare single-particle energies using the $r^2Y_{4,0}$ dependence for the $\lambda = 4$ field †. In this case, the new bare energies are similar to the previous ones, for the low single-particle levels. The three higher proton or neutron level energies are now much closer to the dressed single-particle energies. With this hexadecapole field, perturbation theory is valid at all stages of the minimization procedure in the sense that was mentioned previously.

In all the cases we are able to reproduce the known properties of the one-boson states. In fact, the coupling parameters $\Lambda(\alpha, \lambda)$ do not change sufficiently to alter

† The hexadecapole equilibrium deformations are reproduced using an $r^2Y_{4,0}(\theta, \phi)$ dependence for the hexadecapole field [15]). In such a case, our large matrix elements involving the $\lambda = 4$ phonon vanish, since all of them involve a change in the number of nodes greater than one.

the previous results, if we replace in (5) the bare single-particle energies by the experimental ones. This is shown in table 1, where the values of $\Lambda(\alpha, \lambda)$ are given.

We have attempted to reproduce the single-particle energies by optimizing the potential-depth parameters V_0 and $V_{s.o.}$ in a Saxon-Woods central field,

$$V(r) = -\frac{V_0}{1+\exp((r-R)/a)} + V_{s.o.}\left(\frac{\hbar}{mc}\right)^2 \frac{\exp((r-R)/a)}{2ar} \frac{s\cdot l}{[1+\exp((r-R)/a)]^2}. \tag{7}$$

We have kept the same parameters $a = 0.67$ fm and $R = 1.27\,A^{\frac{1}{3}}$ fm as in ref. [2]). The values of V_0 and $V_{s.o.}$ given in table 4 reproduce (a) the empirical single-particle energies, (b) the bare single-particle energies that are obtained using the r^4 radial dependence for the hexadecapole field and (c) the bare single-particle energies corresponding to the r^2 dependence of the $\lambda = 4$ field.

4. Verification of the wave function

4.1. ONE-BODY TRANSFER PROCESSES

The amount of the admixtures in the single-particle wave functions may be measured by the decrease in the cross sections corresponding to one-body transfer processes. The expression for the spectroscopic amplitudes is

$$\langle km_k|c^+_{km_k}|0\rangle$$
$$= 1 - \frac{1}{2}\frac{2\lambda+1}{2k+1}\sum_{k'}|M(kk',\lambda)|^2\left\{\left(\frac{\Lambda(-2,\lambda)}{W(-2,\lambda)+\varepsilon_k+\varepsilon_{k'}}\right)^2 + \left(\frac{\Lambda(0,\lambda)}{W(0,\lambda)+\varepsilon_{k'}-\varepsilon_k}\right)^2\right\}$$
$$- \frac{1}{2}\frac{2\lambda+1}{2k+1}\sum_{i}|M(ki,\lambda)|^2\left\{\left(\frac{\Lambda(2,\lambda)}{W(2,\lambda)-\varepsilon_i-\varepsilon_k}\right)^2 + \left(\frac{\Lambda(0,\lambda)}{W(0,\lambda)-\varepsilon_i+\varepsilon_k}\right)^2\right\}. \tag{8}$$

In practice, the experimental evaluation of (8) is complicated due to uncertainties in the value of the parameters determining, for instance, the neutron well and the deuteron and proton channels, and in the form of the corrections to the DWBA (lower cut-off radii, finite range and non-local effects, etc.). Up to 1969 [ref. [11])], similar spectroscopic factors were derived from the stripping cross sections to the

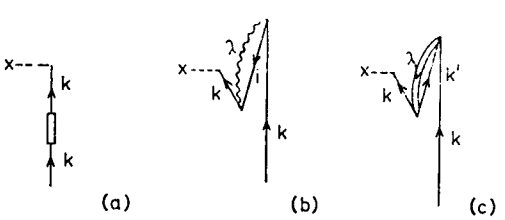

Fig. 2. The graphs represent the three different processes entering in the one-body transfer reactions. The first one corresponds to renormalizations of the single-particle states.

TABLE 5a

The predicted spectroscopic factors for one-neutron stripping and pick-up reactions on ^{208}Pb

l_j	Exp single-particle energies	Bare single-particle energies	
		$r^4Y_{4,0}$ $\Delta W(2, 8) = 0.05$ MeV	$r^2Y_{4,0}$ $\Delta W(2, 8) = 0.05$ MeV
		^{208}Pb → ^{209}Pb	
$g_{\frac{9}{2}}$	0.72	0.78	0.77
$i_{\frac{11}{2}}$	0.86	0.88	0.87
$j_{\frac{15}{2}}$	0.57	0.31	0.31
$d_{\frac{5}{2}}$	0.59	0.63	0.61
$s_{\frac{1}{2}}$	0.46	0.83	0.84
$g_{\frac{7}{2}}$	0.63	0.62	0.59
$d_{\frac{3}{2}}$	0.50	0.05	0.54
		^{208}Pb → ^{207}Pb	
$p_{\frac{1}{2}}$	1.34	1.46	1.46
$f_{\frac{5}{2}}$	4.38	4.62	4.44
$p_{\frac{3}{2}}$	2.60	2.88	2.80
$i_{\frac{13}{2}}$	11.06	11.76	11.62
$f_{\frac{7}{2}}$	4.00	0.72	1.44
$h_{\frac{9}{2}}$	4.56	2.79	2.04

The different listed values have been obtained by replacing in (8) the experimental single-particle energies or the bare single-particle energies corresponding to the hexadecapole fields with the r^4 radial dependence ($\Delta W(2, 8) = 0.05$ MeV) and with the r^2 radial dependence ($\Delta W(2, 8) = 0.05$ MeV), respectively.

TABLE 5b

The same as 5a but for the one-proton transfer reactions

l_j	Exp single-particle energies	Bare single-particle energies	
		$r^4Y_{4,0}$ $\Delta W(2,8) = 0.05$ MeV	$r^2Y_{4,0}$ $\Delta W(2, 8) = 0.05$ MeV
		^{208}Pb → ^{209}Bi	
$h_{\frac{9}{2}}$	0.86	0.88	0.87
$f_{\frac{7}{2}}$	0.76	0.78	0.77
$i_{\frac{13}{2}}$	0.74	0.69	0.72
$f_{\frac{5}{2}}$	0.47	0.21	0.27
$p_{\frac{3}{2}}$	0.44	0.01	0.06
$p_{\frac{1}{2}}$	0.05	0.06	0.10
		^{208}Pb → ^{207}Tl	
$s_{\frac{1}{2}}$	1.50	1.58	1.58
$d_{\frac{3}{2}}$	3.12	3.20	3.12
$h_{\frac{11}{2}}$	10.08	10.44	10.32
$d_{\frac{5}{2}}$	3.96	3.12	0.36
$g_{\frac{7}{2}}$	2.96	1.84	3.36

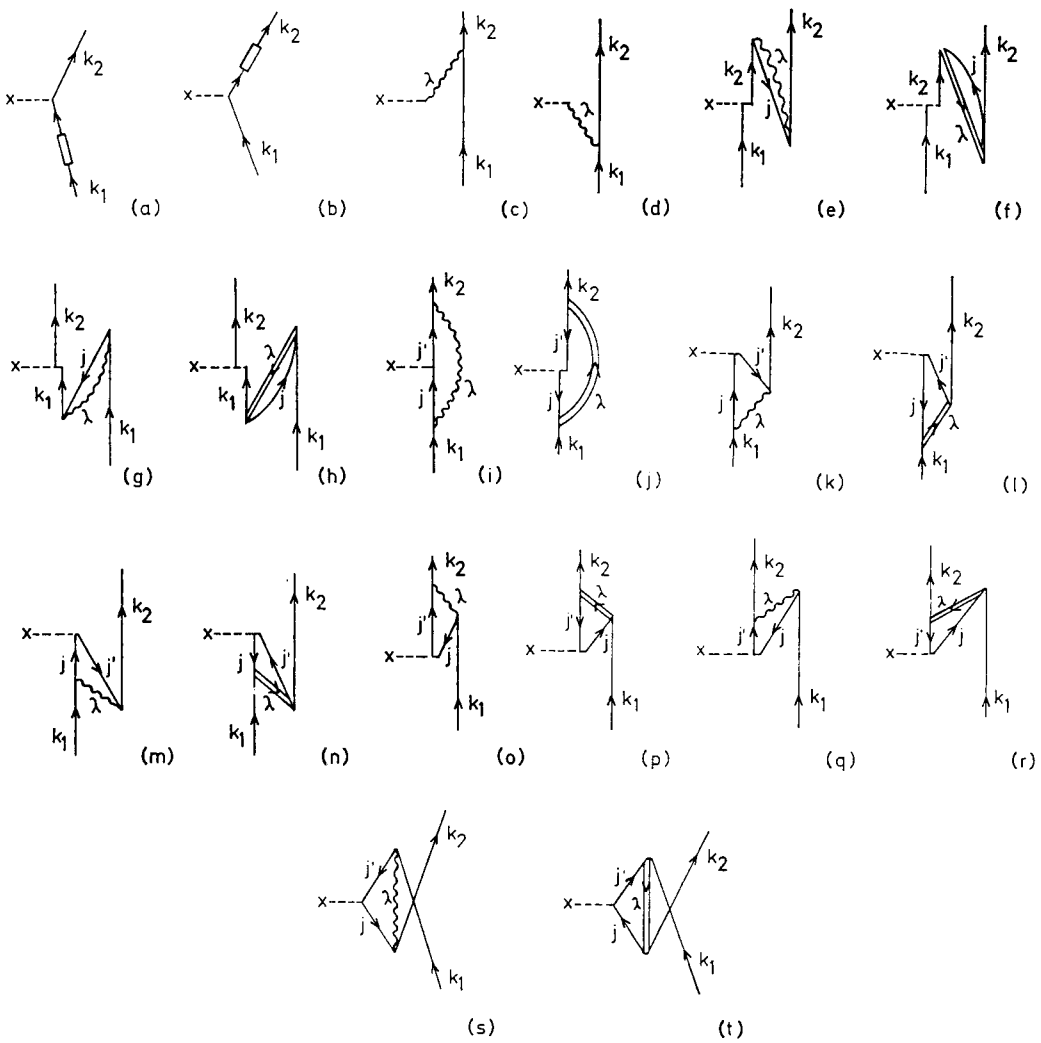

Fig. 3. The graphs used in the calculation of electromagnetic transition rates. The rectangles inserted in the arrows represent renormalization effects.

seven single-neutron states in ^{209}Pb. Since that year, a significant decrease in the spectroscopic factor corresponding to the $\frac{1}{2}^-$ state has been reported [12]). For instance, Vigdor *et al.* [12]) give the spectroscopic factors 1.06 ($g_{\frac{9}{2}}$), 0.97 ($h_{\frac{11}{2}}$), 0.65 ($j_{\frac{15}{2}}$), 1.06 ($d_{\frac{3}{2}}$), 1.13 ($s_{\frac{1}{2}}$), 1.12 ($g_{\frac{7}{2}}$) and 1.05 ($d_{\frac{5}{2}}$).

As a result of our calculation (table 5), the predominantly $s_{\frac{1}{2}}$ and $d_{\frac{3}{2}}$ states should present spectroscopic factors considerable smaller than unity (r^4 dependence of the hexadecapole field), or close to unity (r^2 dependence of the hexadecapole field). Thus, the latter dependence appears to be experimentally favoured.

However (and bearing in mind the previous history of the empirical spectroscopic factors), it is difficult to make a definite statement. For instance, some of the corrections to the DWBA (like IEA) tend to depress the wave functions inside the nucleus and, consequently, they may affect differently the population of states with different number of nodes. Therefore, the evidence concerning the relative population of $g_{\frac{9}{2}}$, $h_{\frac{11}{2}}$ and $j_{\frac{15}{2}}$ states is much more firm than the evidence regarding the spectroscopic factors corresponding to the low angular momentum states.

Another way of exploring the wave functions by one-body transfer processes is to locate the intensity that is missing from the predominantly single-particle states [4]). However the available experimental results do not allow one to extract a definite conclusion from the corresponding analysis, which is not attempted here since a proper calculation involves the admixture of continuous states [4]).

TABLE 6

The values of the effective nucleon charges in units of the proton bare charge

	Initial	Final	Exp single-particle energies	Bare single-particle energies	
				$r^4Y_{4,0}$ $\Delta W(2, 8) = 0.05$ MeV	$r^2Y_{4,0}$ $\Delta W(2, 8) = 0.05$ MeV
Neutron states	$d_{\frac{5}{2}}$	$g_{\frac{9}{2}}$	0.77	0.57	0.50
	$s_{\frac{1}{2}}$	$d_{\frac{5}{2}}$	0.42	0.47	0.37
	$f_{\frac{7}{2}}$	$p_{\frac{1}{2}}$	0.93	0.62	0.62
	$p_{\frac{3}{2}}$	$p_{\frac{1}{2}}$	0.74	0.52	0.47
	average		0.71	0.54	0.49
	rms deviation		0.19	0.06	0.09
Proton states	$f_{\frac{7}{2}}$	$h_{\frac{9}{2}}$	3.58	1.61	1.59
	$f_{\frac{5}{2}}$	$h_{\frac{9}{2}}$	2.64	1.89	2.17
	$p_{\frac{3}{2}}$	$f_{\frac{7}{2}}$	1.98	1.96	1.47
	$d_{\frac{3}{2}}$	$s_{\frac{1}{2}}$	2.32	1.27	1.25
	average		2.63	1.68	1.62
	rms deviation		0.60	0.27	0.34

The predicted transition rates are obtained by replacing in the equations of the appendix the experimental or the bare single-particle energies.

The evidence concerning spectroscopic factors in ^{207}Pb, ^{207}Tl and ^{209}Pb is even less conclusive. For instance, Vigdor *et al.* [12]) report the spectroscopic factors for the pick-up of one neutron [2.22 ($p_{\frac{1}{2}}$), 6.22 ($f_{\frac{7}{2}}$) and 4.05 ($p_{\frac{3}{2}}$)] which are in reasonable agreement with those of table 5a.

4.2. ELECTROMAGNETIC TRANSITION RATES

The present description of the predominantly single-particle states may be further tested by studying the electromagnetic transitions between these states. The corrections to the pure single-particle values are represented in fig. 3.

We must calculate first the matrix elements of the electromagnetic multipole operators between the eigenfunctions of a Saxon-Woods central potential. The Saxon-Woods parameters are given in table 4.

The graphical perturbation treatment introduces two main corrections to the bare operators, acting in opposite directions. The first one tends to decrease the transition rate because of the decrease of the single-particle amplitude (normalization coefficient, see figs. 3a and 3b). The second important contribution is made through the particle-phonon state which may be admixed in the predominantly single-particle state. Its contribution is obtained by multiplying by the factor $\Lambda(0, \lambda)/\chi(0, \lambda)$ the value of the vertex of figs. 3c and 3d (see appendix).

The resultant $B(\mathrm{E2})_{\mathrm{th}}$ values are obtained in units of the electric charge. By comparing with the experimental values we obtain the value of the effective electric charge; table 6 shows four neutron and four proton transitions between predominantly single-particle states. We see that the value of the quadrupole effective charge decreases (as it should) when we take explicitly into account through the perturbation procedure the effects associated with the (0, 2) 4.07 MeV phonon.

Moreover, we see that the rms deviations from the mean value are considerably smaller when we explicitly take into account this phonon, and that the polarization charge is the same for both protons and neutrons within the rms deviations. There is no significant difference between the results corresponding to the use of the experimental energies from those obtained using the bare single-particle energies. The calculations reported in column 1 of table 6 reproduce the results of ref. [3]); those of column 2, refs. [4, 13]). The fact that the neutron and proton polarization charges appear to be the same is somewhat disturbing because of the possible existence of a $T = 1$ giant quadrupole resonance.

5. Comparison with previous calculations

In the paper, we have studied the modification of the single-particle states which are produced through admixtures with collective states of normal parity. (Thus, the relevant admixtures for M1 matrix elements are excluded from this calculation.) Most of the previous papers which involve the same limitation discuss only the 2p-1h or 2h-1p states.

Hamamoto [15]) discusses in detail the admixture of the $(g_{\frac{9}{2}}3^-)^{\frac{15}{2}}$ state in the $j = \frac{15}{2}^-$ single-neutron state and of the $(h_{\frac{9}{2}}3^-)^{\frac{13}{2}}$ state in the $i = \frac{13}{2}^-$ single-proton state. Our results are in substantial agreement with hers in this respect. She also gives the value of 0.13 [0.14] for the $s_{\frac{1}{2}}$ [$p_{\frac{1}{2}}$] admixture probability in the $(g_{\frac{9}{2}}4^+)^{\frac{1}{2}}$ [$(h_{\frac{9}{2}}4^+)^{\frac{1}{2}}$] states. This number is to be compared with our admixture probability of 0.26 [0.36] of the 2p-1h $(g_{\frac{9}{2}}4^+)^{\frac{1}{2}}$ [$(h_{\frac{9}{2}}4^+)^{\frac{1}{2}}$] in the $s_{\frac{1}{2}}$ [$p_{\frac{1}{2}}$] single-neutron [proton] state that is obtained with the r^4 radial dependence, or with the value 0 which is obtained with the r^2 radial dependence. This comparison indicates that the radial derivative of the Saxon-Woods

potential gives results which lie in between those corresponding to our two radial dependences.

As earlier mentioned, a difference between this calculation and those of refs. [4,15]) lies in the fact that we include the pairing phonons (following refs. [7,8])). However in ref. [7]) only one particle-hole phonon (3^-) is included, and the discussion concerning the predominantly single-neutron states in ^{209}Pb is centered on the two-body transfer reactions populating these states. In particular, it is shown that the cross sections to the pure $j^\pi = \frac{15}{2}^-$ state or to a state having an appreciable admixture os the $(g_{\frac{9}{2}}3^-)^{\frac{15}{2}}$ component are predicted to have very similar values. Because of thif lack of sensitivity, we have not included two-body transfer calculations in this paper.

Ref. [16]) includes very similar effects to those treated in this paper, within the framework of the Migdal theory for finite Fermi systems. In both papers, values of the effective charge for the quadrupole transitions are obtained. However the results are difficult to compare, since it is not possible to separate in ref. [16]) the effects which are produced by the giant quadrupole resonances (which are ultimately responsible for our final effective charges of table 6) with those associated with the low energy phonons (which are explicitly taken into account in this calculation).

6. Conclusions

We have eliminated those renormalizations of single-particle parameters that are produced by the lowest phonon states. However, due to uncertainties in the radial dependence of the fields (mainly in the $\alpha = 0$, $\lambda = 4$ component) we are left with two groups of results, corresponding to the r^4 and r^2 dependences of the hexadecapole field, respectively. Each group of bare single-particle energies is adequately reproduced by an appropriate choice of the potential depth parameters in a Saxon-Woods central field.

In order to distinguish between the two possibilities, we have looked at the evidence in spectroscopic factors. This information favours the r^2 dependence, which is characterized by the fact that the spectroscopic factors of the excited single-particle states that can be mixed with the lowest states plus an hexadecapole $\alpha = 0$ phonon, is closer to unity. However, we feel that the present knowledge about the stripping process makes this evidence not fully conclusive.

The electromagnetic E2 transition rates are not very sensitive to the differences between the two groups of bare energies. We find that the values of the effective charges have a considerably smaller spread, once the effects associated with the lower phonons are removed.

Discussions with R. Broglia, G. G. Dussel, E. E. Maqueda and R. P. J. Perazzo are kindly acknowledged.

Appendix

In this appendix we give the matrix elements $\langle c_{k_2}^+|\{Q, c_{k_1}^+\}^{k_2}\rangle$ corresponding to the graphs of fig. 3. We denote by $q(jj')$ the reduced matrix elements of the quadrupole operator between the single-particle eigenstates of the Saxon-Woods central field. They differ from $M(jj', 2)$ by the fact that the last reduced matrix elements are calculated in harmonic oscillator bases (eq. (4)). The matrix elements are as follows:

$$\langle c_{k_2}^+|\{Q, c_{k_1}^+\}^{k_2}\rangle = \frac{q(k_1 k_2)}{\sqrt{2k_2+1}}(1-\tfrac{1}{2}a_1^2-\tfrac{1}{2}a_2^2) \quad \text{(figs. 3a, 3b)},$$

$$\langle c_{k_2}^+|\{Q, c_{k_1}^+\}^{k_2}\rangle = -\frac{5\Lambda^2(0,2)M(k_1 k_2, 2)}{\sqrt{2k_2+1}\,\chi(0,2)}\left(\frac{1}{\varepsilon_{k_2}-\varepsilon_{k_1}-W(0,2)}-\frac{1}{\varepsilon_{k_2}-\varepsilon_{k_1}+W(0,2)}\right)$$

(figs. 3c, 3d),

$$\langle c_{k_2}^+|\{Q, c_{k_1}^+\}^{k_2}\rangle = -\frac{q(k_1 k_2)}{\sqrt{2k_2+1}}\sum_{j\alpha\lambda}(2\lambda+1)\Lambda^2(\alpha,\lambda)\left(\frac{M^2(k_2 j,\lambda)}{(2k_2+1)\{\varepsilon_{k_2}+\varepsilon_j+W(\alpha,\lambda)\}}\right.$$

$$\left.+\frac{M^2(k_1 j,\lambda)}{(2k_1+1)\{\varepsilon_{k_1}+\varepsilon_j+W(\alpha,\lambda)\}}\right) \text{ (figs. 3e–3h)},$$

$$\langle c_{k_2}^+|\{Q, c_{k_1}^+\}^{k_2}\rangle = -\frac{1}{\sqrt{2k_2+1}}\sum_{jj'\alpha\lambda}(2\lambda+1)\Lambda^2(\alpha,\lambda)q(j'j)\begin{Bmatrix}2 & j & j'\\ \lambda & k_2 & k_1\end{Bmatrix}$$

$$\times\frac{M(k_1 j,\lambda)M(j'k_2,\lambda)}{\{\varepsilon_{k_1}-\varepsilon_j-W(\alpha,\lambda)\}\{\varepsilon_{k_2}-\varepsilon_{j'}-W(\alpha,\lambda)\}} \text{ (figs. 3i, 3j)},$$

$$\langle c_{k_2}^+|\{Q, c_{k_1}^+\}^{k_2}\rangle = \frac{1}{\sqrt{2k_2+1}}\sum_{jj'\alpha\lambda}(2\lambda+1)\Lambda^2(\alpha,\lambda)q(j'j)\begin{Bmatrix}2 & j & j'\\ \lambda & k_2 & k_1\end{Bmatrix}$$

$$\times\frac{M(j'k_2,\lambda)M(k_1 j,\lambda)}{\{\varepsilon_{k_1}-\varepsilon_j-W(\alpha,\lambda)\}\{\varepsilon_{k_1}-\varepsilon_{k_2}-\varepsilon_j-\varepsilon_{j'}\}} \text{ (figs. 3k, 3l)},$$

$$\langle c_{k_2}^+|\{Q, c_{k_1}^+\}^{k_2}\rangle = -\frac{1}{\sqrt{2k_2+1}}\sum_{jj'\alpha\lambda}(2\lambda+1)\Lambda^2(\alpha,\lambda)q(jj')\begin{Bmatrix}2 & j & j'\\ \lambda & k_2 & k_1\end{Bmatrix}$$

$$\times\frac{M(j'k_2,\lambda)M(k_1 j,\lambda)}{\{\varepsilon_{k_2}+\varepsilon_{j'}+W(\alpha,\lambda)\}\{\varepsilon_{k_1}-\varepsilon_{k_2}-\varepsilon_j-\varepsilon_{j'}\}} \text{ (figs. 3m, 3n)},$$

$$\langle c_{k_2}^+|\{Q, c_{k_1}^+\}^{k_2}\rangle = \frac{1}{\sqrt{2k_2+1}}\sum_{jj'\alpha\lambda}(2\lambda+1)\Lambda^2(\alpha,\lambda)q(jj')\begin{Bmatrix}2 & j & j'\\ \lambda & k_2 & k_1\end{Bmatrix}$$

$$\times\frac{M(j'k_2,\lambda)M(k_1 j,\lambda)}{\{\varepsilon_{k_2}-\varepsilon_{j'}-W(\alpha,\lambda)\}\{\varepsilon_{k_2}-\varepsilon_{k_1}-\varepsilon_j-\varepsilon_{j'}\}} \text{ (figs. 3o, 3p)},$$

$$\langle c_{k_2}^+ | \{Q, c_{k_1}^+\}^{k_2} \rangle = \frac{1}{\sqrt{2k_2+1}} \sum_{jj'\alpha\lambda} (2\lambda+1) \Lambda^2(\alpha, \lambda) q(j'j) \begin{Bmatrix} 2 & j & j' \\ \lambda & k_2 & k_1 \end{Bmatrix}$$

$$\times \frac{M(j'k_2, \alpha_j M(k_1 j, \lambda)}{\{\varepsilon_{k_1} + \varepsilon_j + W(\alpha, \lambda)\}\{\varepsilon_j + \varepsilon_{j'} + \varepsilon_{k_1} - \varepsilon_{k_2}\}} \quad \text{(figs. 3q, 3r),}$$

$$\langle c_{k_2}^+ | \{Q, c_{k_1}^+\}^{k_2} \rangle = \frac{1}{\sqrt{2k_2+1}} \sum_{jj'\alpha\lambda} (2\lambda+1) \Lambda^2(\alpha, \lambda) q(jj') \begin{Bmatrix} 2 & j' & j \\ \lambda & k_2 & k_1 \end{Bmatrix}$$

$$\times \frac{M(k_1 j', \lambda) M(jk_2, \lambda)}{\{\varepsilon_{k_2} + \varepsilon_j + W(\alpha, \lambda)\}\{\varepsilon_{k_1} + \varepsilon_{j'} + W(\alpha, \lambda)\}} \quad \text{(figs. 3s, 3t).}$$

References

1) N. Stern, Proc. Int. Conf. on properties of nuclear states, Montreal, 1969 (Les Presses de L'Université de Montreal, Montreal, 1969) p. 337
2) J. Blomqvist and S. Wahlborn, Ark. Fys. **16** (1960) 545
3) G. Astner, I. Bergström, J. Blomqvist, B. Fant and K. Wikström, Nucl. Phys. **A182** (1972) 219
4) I. Hamamoto, Nucl. Phys. **A205** (1973) 225, and references therein
5) V. Gillet, B. Giraud and M. Rho, Nucl. Phys. **A103** (1967) 241;
D. R. Bès and G. G. Dussel, Nucl. Phys. **A135** (1969) 1
6) W. Ogle, S. Wahlborn, R. Piepenbring and S. Fredriksson, Rev. Mod. Phys. **43** (1971) 424;
R. R. Chasman, Nucl. Phys. **A89** (1966) 11
7) E. Flynn, G. Igo, P. D. Barnes, D. Kovar, D. R. Bès and R. A. Broglia, Phys. Rev. **C3** (1971) 2371
8) D. R. Bès and R. A. Broglia, Phys. Rev. **C3** (1971) 2349
9) B. R. Mottelson, J. Phys. Soc. Jap. Suppl. **24** (1968) 87
10) R. A. Broglia, V. Paar and D. R. Bès, Phys. Lett. **37B** (1971) 159
11) G. Muehllenhner, A. S. Poltorak, W. C. Parkinson and R. H. Bassel, Phys. Rev. **159** (1967) 1039;
A. F. Jeans, W. Dancey, W. G. Danies, K. N. Jones and P. K. Smith, Nucl. Phys. **A128** (1969) 224
12) C. Ellegaard, J. Kantele and P. Vedelsby, Nucl. Phys. **A129** (1969) 113;
G. J. Igo, P. D. Barnes, E. R. Flynn and D. D. Armstrong, Phys. Rev. **177** (1969) 1831;
S. E. Vigdor, R. D. Rathnell, H. S. Liers and W. Haeberli, Nucl. Phys. **A210** (1973) 70
13) R. A. Broglia, J. S. Lilley, R. Perazzo and W. R. Phillips, Phys. Rev. **C1** (1970) 1508
14) S. G. Nilsson, C. F. Tsang, A. Sobiczewski, Z. Szymański, S. Wycech, C. Gustafson, I. L. Lamm, P. Möller and B. Nilsson, Nucl. Phys. **A131** (1969) 1
15) I. Hamamoto, Nucl. Phys. **A141** (1970) 1
16) P. Ring, R. Baver and J. Speth, Nucl. Phys. **A206** (1973) 97